International Journal of Technology



http://ijtech.eng.ui.ac.id

Research Article

Sensitivity Enhancement of Fiber Bragg Grating-Based Hydrophone Using an Acoustic Resonator for Underwater Sensing

Irwan Rawal Husdi^{1,2}, Andi Setiono², Hari Pratomo², Imam Mulyanto², Mohamad Syahadi^{2,3}, Bambang Widiyatmoko², Retno Wigajatri Purnamaningsih^{1,*}

Abstract: Fiber optic-based hydrophones have many advantages over the piezoelectricbased hydrophones that are commonly used today. Fiber optic-based hydrophones include using fiber Bragg grating (FBG), which has been successfully demonstrated and continues to be developed. However, so far, the sensitivity of FBG-based hydrophones is still relatively low, at around 91 nm/MPa. In this study, a new method is proposed to increase the sensitivity of FBG-based hydrophones using an acoustic resonator. The experiment was conducted using an acoustic resonator in the form of a quarter-wavelength resonator with a fundamental frequency of 2057 Hz. The results of initial experiments on a laboratory scale show that the acoustic signal detected by the proposed FBG-based hydrophone has the same frequency as the sound wave signal generated by an underwater speaker. However, there is a phase difference between the two signals caused by the delay between the sound wave signal generation and hydrophone detection. Experiments using an acoustic resonator in the frequency range of 100 Hz - 4000 Hz showed an increase in sound pressure amplitude, with a maximum sensitivity enhancement of up to 23 dB when the distance between the FBG and the underwater speaker was 5 cm and the sound frequency was 900 Hz.

Keywords: Acoustic resonator; Fiber bragg grating; Fiber optic sensor; Hydrophone sensitivity; Underwater acoustic

1. Introduction

A hydrophone is a sensor used to detect underwater acoustic signals. Considering that around 71% of the Earth's surface is composed of oceans (Visbeck, 2018), the use of hydrophones is very useful and diverse, including for fishing (Rowell et al., 2017; Holt, 2008), marine oil exploration (Cui and Khoo, 2018; K. Wang et al., 2011), tsunami detection (H. Matsumoto et al., 2016; Okal et al., 2007), earthquake detection (Guardato et al., 2023), search and rescue (Pavlidi and Skarsoulis, 2021; Zhao et al., 2017), and even to maintain maritime sovereignty (Parry, 2019). Hydrophones have also been successfully

¹Optoelectronics Laboratory, Department of Electrical Engineering, Universitas Indonesia, Depok 16425, West Java, Indonesia

²Research Center for Photonics, National Research and Innovation Agency, South Tangerang 15314, Banten, Indonesia

³Optical Sensors and Smart Integrated Systems Research Team, LAAS-CNRS, 31031 Toulouse, France *Corresponding author's email: retno.wigajatri@ui.ac.id; Tel.: +62-21-7270078; Fax.:+62-21-7270078

used in field trials to detect blast fishing (Showen et al., 2018; Braulik et al., 2017). Blast fishing is a destructive fishing method that uses explosives to stun or kill fish for easy collection. Remote and real-time detection of blast fishing using hydrophones is very effective for monitoring, considering the vastness of coral reefs, which are usually where blast fishing is carried out. Damage to coral reefs can be avoided, which requires decades or even hundreds of years to recover (Hampton-Smith et al., 2021).

The hydrophone's working principle is based on the interaction between the sensor and the sound pressure generated by sound waves moving in the water. Most hydrophones still use piezoelectric (Saheban and Kordrostami, 2021). However, there are several disadvantages, including large size, sensitivity to electromagnetic interference, and corrosion. Fiber optic-based hydrophones have been developed to overcome these disadvantages (Meng et al., 2021). The use of fiber optics for hydrophones was first reported in 1977 (Bucaro et al., 1977; Cole et al., 1977). Some of the advantages of using fiber optic-based hydrophones when compared to piezoelectric-based hydrophones include immunity to electromagnetic interference and resistance to corrosion (Takahashi et al., 2000), as well as stability in harsh environments and multiplexing capability (Kumar et al., 2021).

The use of fiber Bragg grating (FBG) as a sensor is among the various developments of fiber optic-based hydrophones (Saheban and Kordrostami, 2021). In 1997, the first FBG-based hydrophone was successfully demonstrated in 1997 (Takahashi et al., 1997). However, the use of FBG-based hydrophones still faces several obstacles, including a level of sensitivity that is still lacking for operational use. Using the intensity modulation-based measurement method, the maximum sensitivity obtained was 91.29 nm/MPa (Li et al., 2019).

Several methods have been proposed to improve the sensitivity of FBG-based hydrophones, including using polymer-coated FBG (Moccia et al., 2012; Campopiano et al., 2009), equivalent phase shift FBG with a circle metal disk (Saxena et al., 2012; Huang et al., 2011), clad-etched FBG (Chang et al., 2018), clad-etched FBG with silicon rubber (Liu et al., 2022), and clad-etched FBG with a special package (Sebastian et al., 2022; Prasad et al., 2021). Furthermore, the use of stainless steel-coated FBG results in increased sensitivity for detecting very low hydrostatic pressure (Madani et al., 2023).

In the use of hydrophones for certain applications, the hydrophone sensitivity must be enhanced at a certain frequency range. By using the methods mentioned above, enhancing the hydrophone sensitivity at a certain frequency range can be achieved by selecting the right material with certain mechanical properties (such as Young's modulus and Poisson's ratio) and by adjusting the dimensionality of the material used.

In this study, we propose the use of an acoustic resonator in FBG-based hydrophones. To the best of our knowledge, this is the first time that acoustic resonators are used to enhance the sensitivity of FBG-based hydrophones. The advantage of using an acoustic resonator is the ease of obtaining the frequency range needed to enhance the hydrophone sensitivity. The proposed method uses resonance to amplify the amplitude of the sound pressure signal in a certain frequency range, resulting in the hydrophone sensitivity enhancement. Where amplitude amplification occurs at or near the resonant frequency. The resonant frequency can be easily adjusted because it depends merely on the dimensions of the acoustic resonator. It does not depend on the mechanical properties of the material used as a resonator. This method is easy to implement and can be combined with other methods to obtain even better sensitivity.

A quarter wavelength resonator has a simple structure, an excellent sound pressure amplification effect, and a wide resonance bandwidth (Xiao et al., 2023). Therefore, a quarter wavelength resonator is used in this study. The required frequency range is

obtained by adjusting the length of the quarter wavelength resonator used.

2. Metchods

2.1 Experimental setup and apparatus used

Figure 1 shows the experimental setup used in this study. An underwater speaker (Daravoc JX00B) receives a generating signal from a function generator (Rigol DG4202) through an amplifier (Stanley AA-230). The resulting sound waves will cause sound pressure, which will be detected by the sensor. A uniform fiber Bragg grating (Samyon, center wavelength 1575 nm) is used as a sensor to detect acoustic signals, which is part of the hydrophone system. To measure the detected sound pressure, the hydrophone system will work as follows: A tunable laser (Santec TSL 510) light source sends laser light to the FBG through a circulator (Thorlabs 6015-3-FC). Then, the reflected light from the FBG is forwarded to a photodiode (Thorlabs PDA20CS-EC) through the circulator. The output voltage from the photodiode was measured using a 4-channel PC oscilloscope (PicoScope 4424). The output signal of the amplifier is also measured using a 4-channel PC oscilloscope to compare the detected acoustic signal with the sound wave generated signal.

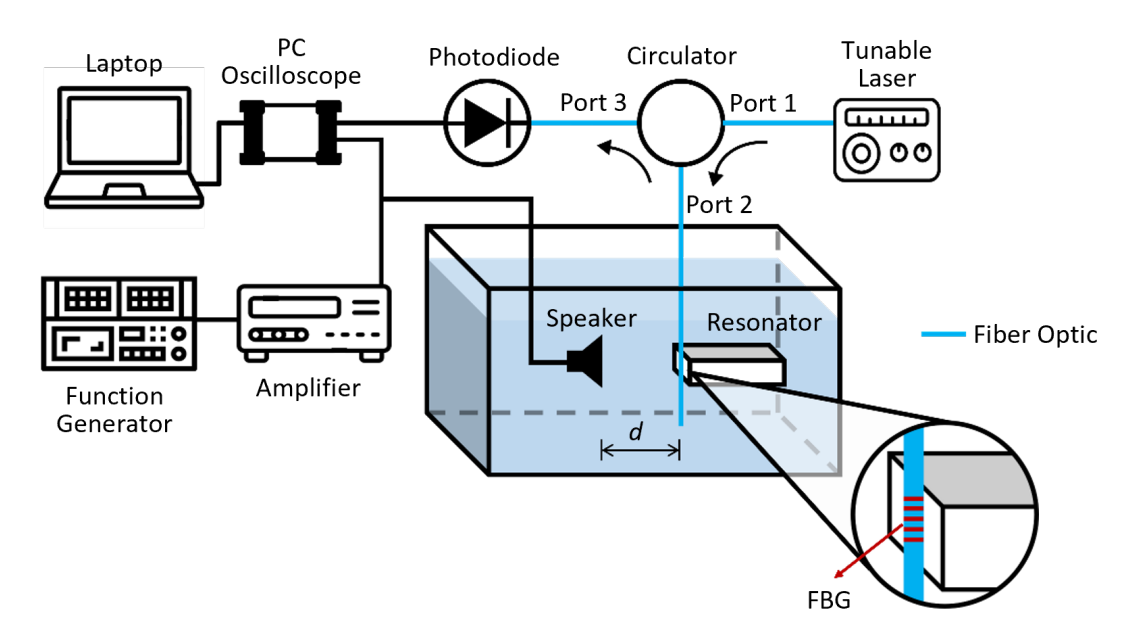


Figure 1 Experimental setup and apparatus consisting of optical and electronic devices and components. d is the distance between the FBG as a sensor and the speaker as a sound source

In this study, the underwater speaker and FBG, which are spaced at a distance of d, are placed in a water tank measuring $100~\rm cm~x~50~cm~x~50~cm$. The proposed method in this study uses an acoustic resonator attached to the FBG sensor. The acoustic resonator was made using polylactic acid (PLA) material. The FBG sensor is attached to the acoustic resonator using a holder.

To minimize the effect of temperature on the measurement results, the experiment was conducted in a controlled laboratory room. Continuous monitoring of the water temperature was conducted during the experiment to avoid significant changes in water temperature. This temperature control also minimizes the possibility of laser wavelength drift. In addition, an inspection was conducted to ensure that the optical connection was

good. In the preliminary measurements, poor optical connections can cause significant harmonics that will affect the accuracy of the measurement.

2.1.1 Acoustic resonator

In this study, an acoustic resonator was used in the form of a quarter-wavelength resonator, which is a square tube with a length of 18 cm. In which one end of the resonator is closed and the other end is open. The FBG sensor is attached to the open end using a holder. Figure 2 shows the used acoustic resonator.

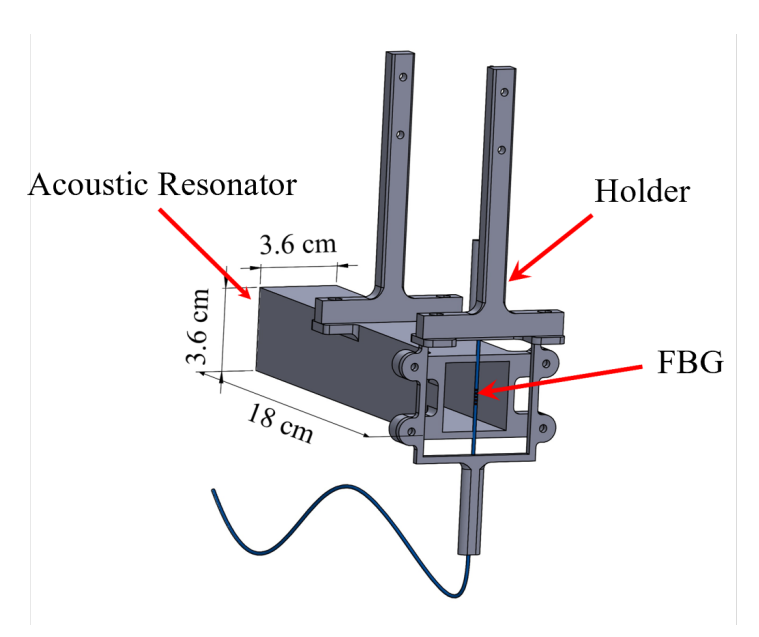


Figure 2 Acoustic resonator with an FBG holder at the open end. L is the length of the acoustic resonator, which is 18 cm

When sound waves enter the resonator, resonance occurs at a certain frequency. A quarter-wavelength resonator has resonant frequencies calculated using the following equation (Catapane et al., 2023):

$$f_{res} = \frac{(2m-1)c_0}{4L} \tag{1}$$

where f_{res} is resonant frequencies, m is an integer, c_0 is the speed of sound, and L is the length of the acoustic resonator. Given that the speed of sound in water is 1481 m/s and L is 18 cm long, the resonator's fundamental frequency (the lowest resonant frequency) is 2057 Hz.

2.2 Interaction between the sound pressure and the FBG

The FBG is characterized by the Bragg wavelength, λ_B , which is defined as the reflection spectrum peak of the FBG. The Bragg wavelength is calculated using the following equation (Xiong et al., 2023):

$$\lambda_B = 2n_{eff} \wedge \tag{2}$$

Where n_{eff} is the effective refractive index of the core, and is the grating period.

When the sound pressure hits the FBG, it causes a shift in the Bragg wavelength due to the photoelastic effect. The change in the Bragg wavelength caused by the photoelastic effect is calculated as follows (X. Wang et al., 2018):

$$\Delta \lambda_B = (1 - p_e)\varepsilon \lambda_B \tag{3}$$

Where p_e is the photoelastic coefficient, is the strain, and λ_B is the Bragg wavelength.

2.3 The sound pressure measurement method

In this study, we performed sound pressure measurements based on the intensity modulation of the reflected light from the FBG. The measurement principle is explained as follows: A tunable laser beam is sent to the FBG. The wavelength of the laser beam was set at the decreasing slope of the FBG reflection spectrum and was close to the Bragg wavelength. As explained earlier, when a sound pressure hits the FBG, it will cause a shift in the Bragg wavelength due to the photoelastic effect. This shift in the Bragg wavelength is followed by a shift in the reflection spectrum. This changes the reflectance coefficient at the wavelength of the laser light. Thus, the intensity of the reflected light changes according to the reflectance coefficient. The change in the intensity of the reflected light is linearly proportional to the sound pressure. With this measurement method, the change in sound pressure will change the reflected light intensity. The intensity of the reflected light will be measured using a photodiode. The photodiode converts the reflected light intensity into a current that is linearly proportional to the reflected light intensity. Furthermore, the current is converted into a photodiode output voltage that is linearly proportional to the current. In summary, the sound pressure is linearly proportional to the photodiode output voltage.

3. Results and Discussion

3.1 FBG-based hydrophone response to the sound pressure

We performed the FBG-based hydrophone response measurement by generating sound waves in the frequency range of 100 Hz-4000 Hz. This frequency range is chosen to match frequencies used for the application of blast fishing detection. In remote detection, most of the blast fishing signals detected by hydrophones consist of signals with frequencies below 5 kHz, because seawater quickly attenuates signals with higher frequencies (Braulik et al., 2015). The frequency used in this study was limited to 4000 Hz. The frequency is gradually changed up to a frequency of 1000 Hz with a frequency interval of 100 Hz and then with a frequency interval of 500 Hz. The experimental results show that the frequency of the signal detected by the FBG-based hydrophone is the same as that of the sound pressure-generated signal. Figure 3 shows the measurement results obtained using the FBG-based hydrophone at frequencies of 500 and 800 Hz. Although they have the same frequency, a phase difference exists between the two signals, which is caused by several factors, including the distance between the speaker and the FBG-based hydrophone, the delay from the function generator to the speaker, and the delay from the FBG to the photodiode. This is in accordance with the results of a previous study in which the detected signal had the same frequency but a different phase from the generated signal (Liu et al., 2022).

Measurements were carried out over a longer period to ensure the similarity of the frequency. Figure 4 shows the measurement results of the generated and detected signals at a period of 0.1 s with a generating signal frequency of 800 Hz. The fast Fourier

transform (FFT) results confirm that the frequencies of the two signals remain the same over longer measurement periods.

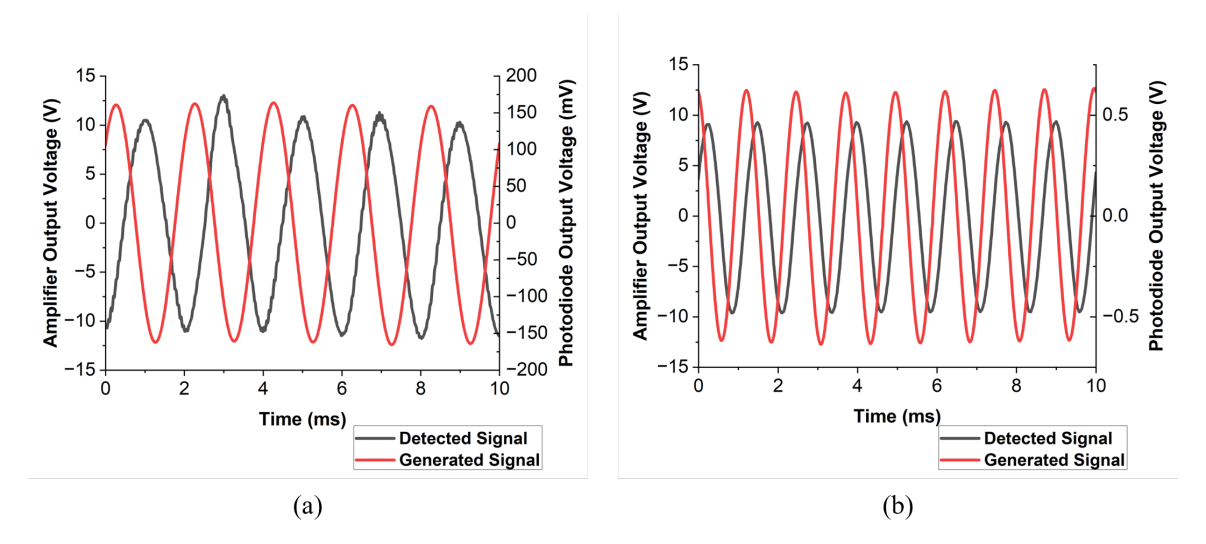


Figure 3 Signal generated from a function generator through an amplifier and the FBG-based hydrophone response measured using a photodiode for (a) f = 500 Hz and (b) f = 800 Hz. The two signals have the same frequency but a different phase due to delays

3.2 Frequency response of the underwater speaker

This study also investigated the frequency response of the underwater speaker. For this purpose, acoustic signal measurements were carried out at 2 different speaker-FBG distances, d. The experiment was carried out at distances, d, of 5 and 10 cm. Measurements were performed using an FBG sensor without an acoustic resonator. Figure 5 shows the results of the photodiode output voltage measurements showing the frequency response of the underwater speaker used.

The underwater speaker output is not constant but varies. Previous studies have also shown that the underwater speaker output varies as a function of frequency (Y. Matsumoto et al., 2022).

3.3 Enhancement of sensitivity using an acoustic resonator

To study the effect of the acoustic resonator on sensitivity, in the next measurement the FBG was placed in the middle of the open end of the acoustic resonator using a holder. Then, measurements were performed without an acoustic resonator by changing the sound frequency in the same range as the previous measurements.

The results of the measurements performed using a resonator were then compared with the results of the measurements without a resonator to determine the effect of the acoustic resonator. Tables 1 and 2 show the measurement results.

The comparison of the two measurement results is represented by the obtained gain. The gain is usually calculated in dB units. For this purpose, the sound pressure level (SPL) is used, expressed in decibels (dB), which is commonly used to describe sound pressure. The SPL is calculated using the following equation (Suedel et al., 2019):

$$L_p = 10log_{10} \frac{p^2}{p_{ref}^2} \tag{4}$$

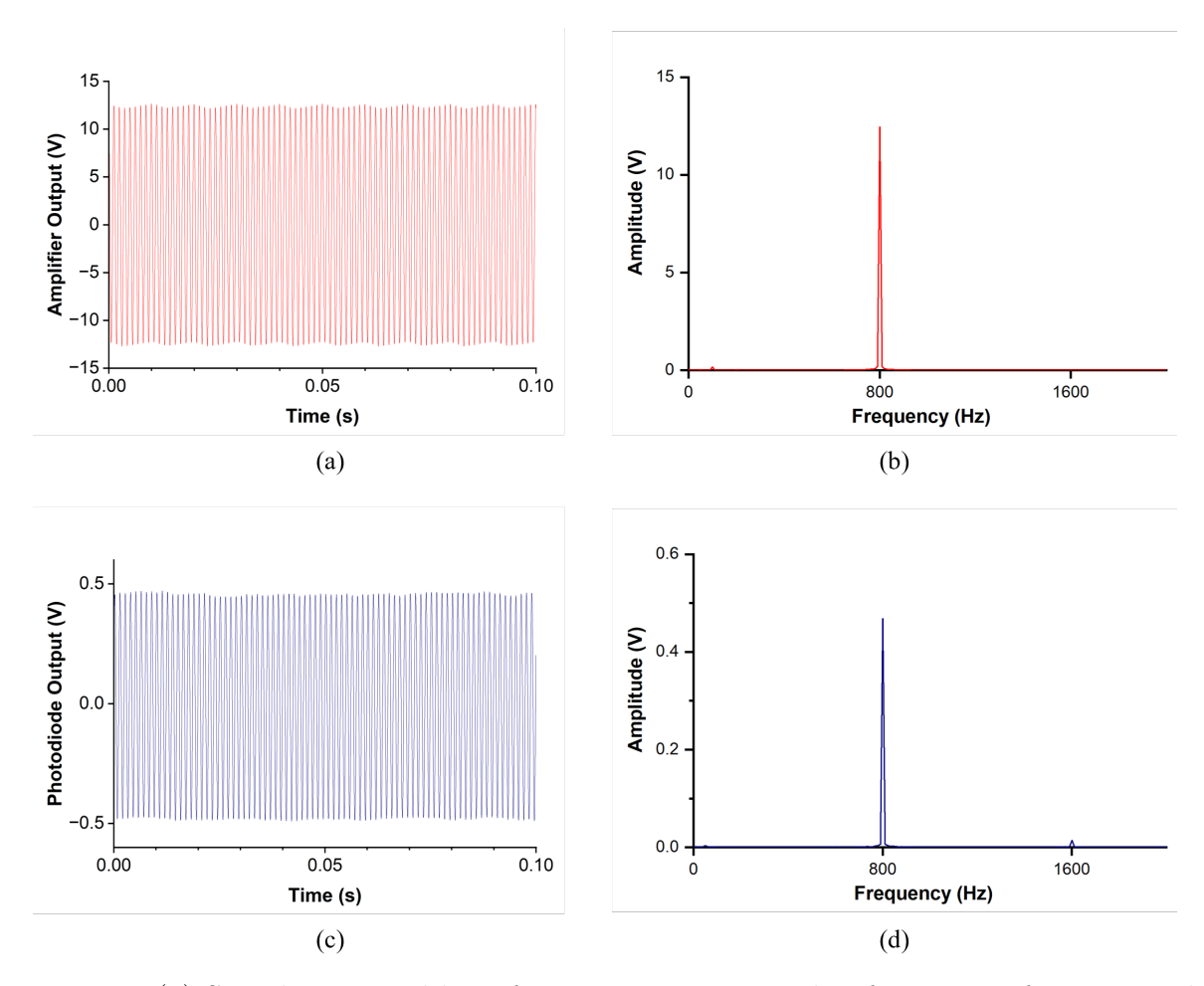


Figure 4 (a) Signal generated by a function generator with a frequency of 800 Hz and (b) its FFT. (c) Signal detected by the FBG-based hydrophone and (d) its FFT. The two signals have the same frequency (800 Hz) for a longer measurement period (0.1 s)

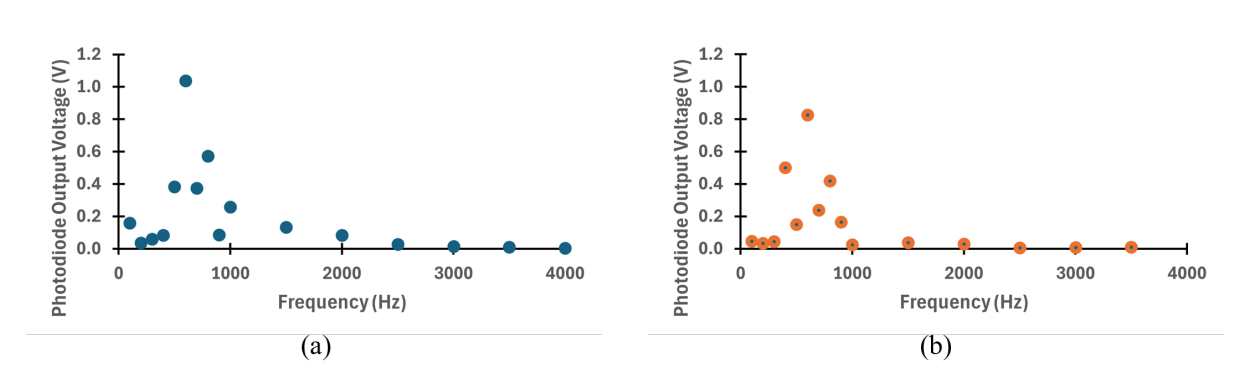


Figure 5 Frequency response of the underwater speaker for a speaker-FBG distance of (a) 5 cm and (b) 10 cm

Where L_p is the SPL expressed in dB, p is the measured sound pressure, and p_{ref} is the reference sound pressure. The reference value for underwater sound pressure is 1 t Pa. Furthermore, the gain, G, is calculated using the following equation:

$$G = L_{pres} - L_{p0} \tag{5}$$

$$G = 20 \frac{p_{res}}{p_0} \tag{5}$$

Table 1 Measurement results of the amplitude of the photodiode output voltage (V_{PD})
without and with the resonator for a distance, d, of 5 cm

Frequency (Hz)	V_{PD} without resonator (mV)	V_{PD} without resonator (mV)
100	159.30	85.10
200	36.85	36.15
300	59.30	30.90
400	83.00	546.55
500	383.05	453.70
600	1037.45	547.75
700	373.95	859.40
800	571.85	546.85
900	86.60	1356.40
1000	285.70	907.10
1500	134.30	316.40
2000	83.25	130.60
2500	28.35	26.85
3000	14.50	47.85
3500	9.95	34.30
4000	4.90	7.00

Table 2 Measurement results of the amplitude of the photodiode output voltage (V_{PD}) without and with the resonator for a distance, d, of 10 cm

Frequency (Hz)	V_{PD} without resonator (mV)	V_{PD} without resonator (mV)
100	46.75	21.47
200	33.10	14.00
300	44.15	7.17
400	502.05	253.60
500	149.35	91.67
600	825.60	121.90
700	237.75	384.50
800	419.15	22.90
900	166.00	137.10
1000	24.75	39.93
1500	38.50	120.97
2000	28.85	69.63
2500	6.95	10.70
3000	8.65	23.90
3500	9.45	7.77
4000	6.40	2.37

Where L_{pres} is the SPL when using a resonator, L_{p0} is the SPL without a resonator. Furthermore, p_{res} is the sound pressure using a resonator, and p_0 is the sound pressure without a resonator.

As explained in the Methods section, the sound pressure is linearly proportional to the photodiode output voltage. Figure 6 shows the gain obtained at a frequency of $100-4000~\rm{Hz}$ for a distance, d, between the underwater speaker and the FBG of 5 and 10 cm.

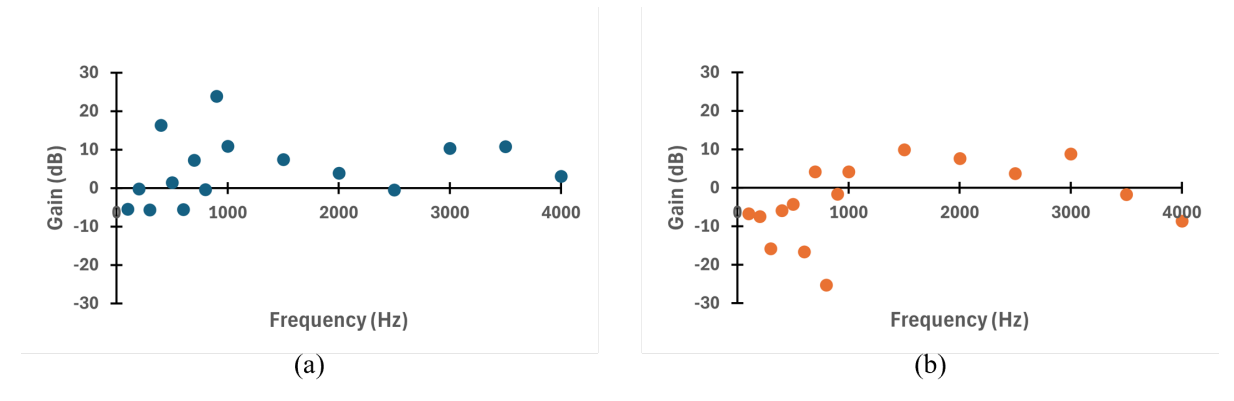


Figure 6 Gain obtained by comparing the response of the FBG-based hydrophone with and without a resonator. (a) Gain obtained for a distance between the FBG and the speaker of 5 cm, and (b) gain obtained for a distance of 10 cm

Figure 6 shows that at certain frequencies, the response of the FBG-based hydrophone using an acoustic resonator is amplified compared with the response of the FBG-based hydrophone without an acoustic resonator. In measurements where the distance between the FBG and the speaker is 5 and 10 cm, it can be seen that in the frequency range studied (100–4000 Hz), especially in the frequency range of 1000 Hz to 3000 Hz, an amplification of the response of the FBG-based hydrophone using an acoustic resonator can be observed. Thus, the sensitivity of the FBG-based hydrophone is enhanced when using an acoustic resonator. The frequency range of 1000 Hz - 3000 Hz, where there is an amplification of the FBG-based hydrophone response for the 2 distances of 5 and 10 cm, is around the fundamental frequency of the acoustic resonator, which is 2057 Hz.

Resonance causes the amplification of the FBG response by the acoustic resonator. Here, resonance depends only on the shape and dimensions of the acoustic resonator and does not depend on the properties of the acoustic resonator material. This is advantageous for measurement stability because the shape and dimensions are relatively more resistant to environmental changes.

4. Conclusion

The results of this study indicate that the proposed FBG-based hydrophone can effectively detect sound pressure, as shown in the measurement results. The signal frequency detected by the FBG-based hydrophone and the signal frequency of the generated sound pressure are the same. In addition, a sensitivity enhancement of the proposed FBG-based hydrophone using an acoustic resonator was successfully observed. Sensitivity enhancement can be observed especially in the frequency range of 1000 Hz-3000 Hz or around the fundamental frequency of the acoustic resonator. The proposed FBG-based hydrophone exhibited a sensitivity enhancement of up to 23 dB at an FBG-speaker distance of 5 cm and a frequency of 900 Hz.

Acknowledgements

The authors would like to thank the Faculty of Engineering, the University of Indonesia, for providing support through the Seed Funding Grant No: NKB-2615/UN2.F4.D /PPM.00.00/2023, and also to thank BRIN for the Grant of Rumah Program ORNM 2024.

Author Contributions

Irwan Rawal Husdi – conceptualization, literature review, experimentation, analysis, manuscript drafting; Andi Setiono – experimentation, review; Hari Pratomo – experimentation, data collection, Imam Mulyanto – experimentation, data collection; Mohamad Syahadi – analysis, review; Bambang Widiyatmoko – conceptualization, experimentation, analysis, review; Retno Wigajatri Purnamaningsih – conceptualization, analysis, review, editing.

Conflict of Interest

The authors declare no conflicts of interest.

References

- Braulik, G., Wittich, A., Macaulay, J., Kasuga, M., Gordon, J., Davenport, T., & Gillespie, D. (2017). Acoustic monitoring to document the spatial distribution and hotspots of blast fishing in tanzania. *Marine Pollution Bulletin*, 125(1-2), 360–366. https://doi.org/https://doi.org/10.1016/j.marpolbul.2017.09.036
- Braulik, G., Wittich, A., Macaulay, J., Gillespie, D., & Davenport, T. (2015). Fishing with explosives in tanzania: Spatial distribution and hotspots. *ResearchGate*. https://doi.org/https://doi.org/10.1016/j.marpolbul.2017.09.036
- Bucaro, J., Dardy, H., & Carome, E. (1977). Fiber-optic hydrophone. The Journal of the Acoustical Society of America, 62(5), 1302–1304. https://doi.org/https://doi.org/10.1121/1.381624
- Campopiano, S., Cutolo, A., Cusano, A., Giordano, M., Parente, G., Lanza, G., & Laudati, A. (2009). Underwater acoustic sensors based on fiber bragg gratings. *Sensors*, 9(6), 4446–4454. https://doi.org/10.3390/s90604446
- Catapane, G., Petrone, G., Robin, O., & Verdière, K. (2023). Coiled quarter wavelength resonators for low-frequency sound absorption under plane wave and diffuse acoustic field excitations. *Applied Acoustics*, 209, 109402. https://doi.org/https://doi.org/10.1016/j.apacoust.2023.109402
- Chang, H.-Y., Kuo, C.-Y., Wang, T.-L., Chang, Y.-C., Fu, M.-Y., & Liu, W.-F. (2018). Hydrophone based on a fiber bragg grating. 2018 Progress In Electromagnetics Research Symposium, 233–236. https://doi.org/10.23919/PIERS.2018.8598171
- Cole, J., Johnson, R., & Bhuta, P. (1977). Fiber-optic detection of sound. *The Journal of the Acoustical Society of America*, 62(5), 1136–1138. https://doi.org/https://doi.org/10.1121/1.381647
- Cui, S., & Khoo, D. (2018). Underwater calibration of hydrophones at very low frequencies from 30 hz to 2 khz. *Journal of Physics: Conference Series*, 1065, 072015. https://doi.org/10.1088/1742-6596/1065/7/072015
- Guardato, S., Riccio, R., Janneh, M., Bruno, F., Pisco, M., Cusano, A., & Iannaccone, G. (2023). An innovative fiber-optic hydrophone for seismology: Testing detection capacity for very low-energy earthquakes. *Sensors*, 23, 3374. https://doi.org/10.3390/s23073374
- Hampton-Smith, M., Bower, D., & Mika, S. (2021). A review of the current global status of blast fishing: Causes, implications and solutions. *Biological Conservation*, 262, 109307. https://doi.org/10.1016/j.biocon.2021.109307

- Holt, S. (2008). Distribution of red drum spawning sites identified by a towed hydrophone array. Transactions of The American Fisheries Society TRANS AMER FISH SOC, 137, 551–561. https://doi.org/10.1577/T03-209.1
- Huang, S., Jin, X., Zhang, J., Chen, Y., Wang, Y., Zhou, Z., & Ni, J. (2011). An optical fiber hydrophone using equivalent phase shift fiber bragg grating for underwater acoustic measurement. *Photonic Sensors*, 1, 289–294. https://doi.org/10.1007/s13320-011-0023-6
- Kumar, H., Sharan, A., & Sreerangaraju, M. N. (2021). Underwater acoustic pressure sensing using optical fiber bragg grating. 2021 8th International Conference on Computing for Sustainable Global Development (INDIACom), 584–590.
- Li, C., Xiaobin, P., Liu, J., Wang, C., Fan, S., & Cao, S. (2019). D-shaped fiber bragg grating ultrasonic hydrophone with enhanced sensitivity and bandwidth. *Journal of Lightwave Technology*, PP, 1–1. https://doi.org/10.1109/JLT.2019.2898233
- Liu, W.-F., Li, J.-G., Chang, H.-Y., Fu, M.-Y., & Chen, C.-F. (2022). A new type of etched fiber grating hydrophone. Photonics, 9(4). https://doi.org/10.3390/photonics9040255
- Madani, N. A., Purnamaningsih, R. W., Poespawati, N. R., Hamidah, M., Rahardjo, S., & Wibowo, D. K. (2023). Detection of low hydrostatic pressure using fiber bragg grating sensor. *International Journal of Technology*, 14(7), 1527–1536. https://doi.org/10.14716/ijtech.v14i7.6714
- Matsumoto, H., Haralabus, G., Zampolli, M., & Özel, N. M. (2016). T-phase and tsunami pressure waveforms recorded by near-source ims water-column hydrophone triplets during the 2015 chile earthquake. *Geophysical Research Letters*, 43(24), 12, 511–12, 519. https://doi.org/https://doi.org/10.1002/2016GL071425
- Matsumoto, Y., Mizushima, Y., & Sanada, T. (2022). Removing gas from a closed-end small hole by irradiating acoustic waves with two frequencies. *Micromachines*, 13(1). https://doi.org/10.3390/mi13010109
- Meng, Z., Chen, W., Wang, J., Hu, X., Chen, M., & Zhang, Y. (2021). Recent progress in fiber-optic hydrophones. *Photonic Sensors*, 11, 109–122. https://doi.org/10.1007/s13320-021-0618-5
- Moccia, M., Consales, Iadicicco, A., Pisco, M., Cutolo, Galdi, V., & Cusano. (2012). Resonant hydrophones based on coated fiber bragg gratings. *JOURNAL OF LIGHT-WAVE TECHNOLOGY*, 30, 2472–2481. https://doi.org/10.1109/JLT.2012.2200233
- Okal, E., Talandier, J., & Reymond, D. (2007). Quantification of hydrophone records of the 2004 sumatra tsunami. *Pure and Applied Geophysics*, 164 (2–3), 309–323. https://doi.org/https://doi.org/10.1007/s00024-006-0165-4
- Parry, J. (2019). An underwater world of walls: Machine sensing, maritime sovereignty, and the aesthetics of undersea surveillance. *Theory & Event*, 22(4), 891–910. https://doi.org/https://doi.org/10.1353/tae.2019.0058
- Pavlidi, D., & Skarsoulis, E. K. (2021). Enhanced pulsed-source localization with 3 hydrophones: Uncertainty estimates. *Remote Sensing*, 13(9). https://doi.org/10.3390/rs13091817
- Prasad, P., Sundarrajan, A., & Nayak, J. (2021). Fiber bragg grating (fbg)-based hydrophone with side-hole packaging for underwater acoustic sensing. *ISSS Journal of Micro and Smart Systems*, 10. https://doi.org/10.1007/s41683-021-00077-2
- Rowell, T., Demer, D., Aburto-Oropeza, O., Cota-Nieto, J., Hyde, J., & Erisman, B. (2017). Estimating fish abundance at spawning aggregations from courtship sound levels open. *Scientific Reports*, 7. https://doi.org/10.1038/s41598-017-03383-8

- Saheban, H., & Kordrostami, Z. (2021). Hydrophones, fundamental features, design considerations, and various structures: A review. Sensors and Actuators A: Physical, 329, 112790. https://doi.org/10.1016/j.sna.2021.112790
- Saxena, I., Guzman, N., & Pflanze, S. (2012). Frequency response comparison of two fbg-based hydrophones. *Proceedings of SPIE The International Society for Optical Engineering*, 8368, 228–. https://doi.org/10.1117/12.923344
- Sebastian, S., Prasad, P., Michael, K., Avaaru, S., & Sundarrajan, A. (2022). Validation of packaged clad-etched fiber bragg grating as underwater acoustic sensor. *IEEE Sensors Journal*, *PP*, 1–1. https://doi.org/10.1109/JSEN.2022.3227461
- Showen, R., Dunson, C., Woodman, G., Christopher, S., Lim, T., & Wilson, S. (2018). Locating fish bomb blasts in real-time using a networked acoustic system. *Marine Pollution Bulletin*, 128, 496–507. https://doi.org/https://doi.org/10.1016/j.marpolbul.2018.01.029
- Suedel, B., McQueen, A., Wilkens, J., & Fields, M. (2019). Evaluating effects of dredging-induced underwater sound on aquatic species: A literature review. *Environmental Review*. https://doi.org/10.21079/11681/34245
- Takahashi, N., Hirose, A., & Takahashi, S. (1997). Underwater acoustic sensor with fiber bragg grating. *Optical Review*, 4(6), 691–694. https://doi.org/https://doi.org/10.1007/s10043-997-0691-z
- Takahashi, N., Yoshimura, K., Takahashi, S., & Imamura, K. (2000). Development of an optical fiber hydrophone with fiber bragg grating. *Ultrasonics*, 38, 581–585. https://doi.org/https://doi.org/10.1016/S0041-624X(99)00105-5
- Visbeck, M. (2018). Ocean science research is key for a sustainable future. *Nature Communications*, 9. https://doi.org/10.1038/s41467-018-03158-3
- Wang, K., Shi, Q., Tian, C., Duan, F., Zhang, M., & Liao, Y. (2011). The design of integrated demodulation system of optical fiber hydrophone array for oceanic oil exploration. In B. Culshaw, Y. Liao, A. Wang, X. Bao, & X. Fan (Eds.), 2011 international conference on optical instruments and technology: Optical sensors and applications (81990R, Vol. 8199). SPIE. https://doi.org/10.1117/12.904035
- Wang, X., Guo, Y., Xiong, L., & Wu, H. (2018). High frequency optical fiber bragg grating accelerometer. *IEEE Sensors Journal*, *PP*, 1–1. https://doi.org/10.1109/JSEN. 2018.2833885
- Xiao, X., Liu, L., Ziyue, X., Yu, H., Li, W., Wang, Q., Zhao, C., Huang, Y., & Xu, M. (2023). Research on an optimized quarter-wavelength resonator-based triboelectric nanogenerator for efficient low-frequency acoustic energy harvesting. *Nanomaterials*, 13, 1676. https://doi.org/10.3390/nano13101676
- Xiong, J., Zhang, W., Song, Y., Wen, K., Zhou, Y., Chen, G., & Zhu, L. (2023). Spectral splitting sensing using optical fiber bragg grating for spacecraft lateral stress health monitoring. *Applied Sciences*, 13, 4161. https://doi.org/10.3390/app13074161
- Zhao, J., Zhang, L., Zheng, L.-n., & Li, N. (2017). The design and research of intelligent search and rescue device based on sonar detection and marine battery. *International Conference on Communications, Network and Embedded Systems (ICC-NEA)*, 383–387. https://doi.org/10.1109/ICCNEA.2017.73